文章编号:1672-6553-2022-20(3)-066-11
DOI:10.6052/1672-6553-2021-040

受轴向激励弹性支承梁的稳定性分析

张弛　毛晓晔　丁虎[†]　陈立群
(上海大学 力学与工程科学学院,上海　200444)

摘要　对于广泛存在的弹性支撑梁,首次呈现支承弹簧刚度对轴向激励下梁横向振动稳定性的影响. 应用 Hamilton 原理,建立了两端由线性弹簧支撑的受轴向激励梁的动力学控制方程. 通过解析方法计算了受轴向压力梁的固有频率,得到了支撑弹簧刚度与系统固有频率和临界轴力的关系. Galerkin 截断后,通过多尺度法和 Runge-Kutta 法,计算得到了梁参激振动稳态响应的半解析与数值解. 讨论了激励幅值、支撑弹簧刚度、平均轴力对系统非线性响应幅值及软硬特性的影响. 利用 Routh-Hurwitz 稳定性判据,求得系统的参激稳定边界,着重讨论了支撑弹簧刚度、阻尼系数的影响. 研究发现,边界支撑弹簧的刚度可以显著改变受轴向激励梁的参激稳定边界. 因此,研究结果将为广泛存在受到轴向激励结构的设计提供指导.

关键词　梁,　弹性支撑,　轴向激励,　参激振动,　非线性振动,　稳定边界
中图分类号:O322　　**文献标志码:**A

引言

弹性支承梁是工程结构中最重要的元件之一,工程中的梁结构与相邻的系统相互作用, 承受载荷,当受到激励作用时,结构的支座弹簧和阻尼可以有效缓解激励作用,提高结构抗力[1,2],采用弹性支承梁可以提高结构稳定性,而且理论上弹性结构的约束也不可能是绝对的刚性支撑,所以弹性支承梁在建筑、桥梁和防护工程中都有广泛的应用 ,如防冲击梁结构[1],以及弹性橡胶支座的桥梁结构[3]. 同时,飞机中的管道结构也可简化为梁模型,这类管道在非定常流或外界激励影响下会发生剧烈振荡,进而损坏[4],这类问题引起了学者们的广泛关注[5,6]. Mao 等[7]研究了超临界条件下,输流管道 3:1 内共振的稳态响应. Tan 等[8-10]采用 Timoshenko 梁模型对输流管道进行了一系列研究. 较早的研究者多将目光集中于轴向运动速度和系统固有频率之间的关系,以及临界流速处的发散失稳上. 这些研究往往都是基于理想化的支承情况,在实际工程中已有使用弹性支承构件减轻结构振动的实例.

1996 年,Kang 和 Kim[11]研究了弹性支承梁和板的模态特性与横向自由振动. 2000 年,夏季和朱目成等人给出了带有多个弹性支承与集中质量的梁的固有频率的精确计算方法[12]. 之后 Li 使用了一种新的方法来分析两端具有任意弹性支承边界梁的模态特性[13],并将其推广到二维问题的研究中[14,15]. 2013 年,Li 等[16]在梁的两端同时加上了扭转弹性约束和竖向弹性支承约束并研究了其对梁固有频率的影响. 2017 年,Gan 等[17]利用有限元建模,研究了中间弹性支承的位置和刚度对动点荷载作用下功能梯度欧拉-伯努利梁振动的影响. 2018 年,Ding 等[18]研究了弹性支承弹性结构的力传递问题并证明了其研究的必要性,之后 Ding 等[19]分析发现弹性边界会对弹性梁非线性特性产生显著的影响. 然而,以上工作大部分是对弹性支承结构的自由振动或是其在横向激励下受迫振动的研究. 近年来关于轴向运动体参激振动的研究受

2021-04-14 收到第 1 稿,2021-05-04 收到修改稿.
∗国家自然科学基金杰出青年项目(12025204)
† 通信作者 E-mail:dinghu3@shu.edu.cn

到广泛关注[20-25],2019 年,Li 等研究了两端带有弹簧支撑的轴向运动梁的特性,分析了弹簧刚度对临界速度的影响,同时通过力传递率研究了系统的隔振效果[26]. 而受轴向力激励的弹性支承梁的相关研究仍然较少.

对于工程中普遍存在的受轴向载荷梁,早在 1975 年,Shaker[27] 就已经分析了轴向载荷对端部带有集中质量均匀悬臂梁固有频率和振型的影响. 到上世纪 90 年代,已有许多相关的研究成果[28-32]. 2000 年,Ji 和 Hansen[33] 对一端固定一端滑动屈曲梁在轴向简谐载荷作用下的非线性响应进行了实验研究,同时还考察了不同阻尼下的不稳定区和混沌响应区. 2004 年,Naguleswaran[34] 研究了均匀欧拉-伯努利梁在沿轴向线性分布全拉伸、部分拉伸和全压缩轴向力作用下的横向振动. 2005 年,Liu 和 Chang[35] 研究了一般边界条件下磁弹性梁在磁力、轴向力和弹簧力作用下的振动. Pratiher 和 Dwivedy[36] 采用多尺度法确定了端部质量悬臂梁在时变磁场和轴向力作用下的参数不稳定区,得到了各个系统参数对参数失稳区域的影响. 2008 年,Yang 等[37] 对含开口边裂纹非均匀欧拉-伯努利梁受轴向压力和沿纵向移动集中横向载荷的自由振动和受迫振动进行了分析研究. 2011 年,Li 等[38] 对具有初始轴向张力简支纳米梁的横向振动展开了研究,发现外部轴向张力和非局部纳米尺度参数对非局域纳米梁的非线性振动行为有重要影响. 2015 年,Li[39] 提出了一种解析方法,并采用该方法和有限元法分别计算了两端铰支梁和两端固定梁在轴向拉力和轴向压力作用下的动力响应,验证了其有效性. 2020 年,Zhou 等[40] 研究了轴向基础激励与内流速度对输液管道非线性受迫振动的联合影响. 同年,Zhao 等[41] 提出了轴向压缩载荷作用下耦合 Timoshenko 双梁系统横向受迫振动的适用于任何边界条件的广义解,并讨论了高长比、剪切效应、转动惯量等物理参数以及轴向压缩载荷的影响. 不过,这些研究中梁都是建立在简支、固支、自由几种典型边界上. 当边界受弹性约束,受到轴向力作用梁的临界屈曲轴力、振动稳定性都可能会发生变化,这对于弹性结构稳定性设计至关重要. 目前尚未有相关研究成果发表.

基于以上调研,本文将重点研究支撑弹簧刚度对受轴向激励弹性支承梁横向非线性振动的影响. 第一节利用 Hamilton 原理建立受轴向激励弹性支承梁的非线性动力学控制方程. 第二节进行模态分析,研究支撑弹簧刚度对系统临界轴力和固有频率的影响. 第三节将使用 Galerkin 法将方程进行截断,得到一系列常微分方程,并进行无量纲化. 第四节利用多尺度法对该参激振动进行近似解析求解,分析激励幅值、支撑刚度、平均轴力等参数对系统非线性响应的影响,然后通过稳定性分析研究支撑弹簧刚度、阻尼系数对系统稳定边界的影响,并进行数值验证. 第五节得到结论.

1　数学模型和控制方程

如图 1 所示,梁的长度为 L,两端弹簧支承刚度分别为 K_L 和 K_R,ρ 为梁的质量密度,A 为横截面面积,E 为弹性模量,I 是梁关于中心轴的横截面惯性矩. 梁受轴向张力 P,该轴向力由平均张力 P_0 与脉动张力 P_1 组成.

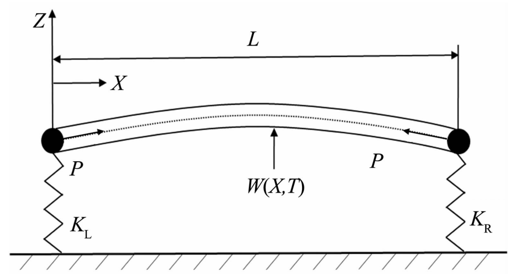

图 1　受轴向激励弹性支撑梁物理模型
Fig. 1　The model of axially excited beam with elastic boundaries

利用 Hamilton 原理建立系统运动控制方程

$$\int_{T_1}^{T_2}(-\delta T_k + \delta V_p + \delta V_s)\,\mathrm{d}T = 0 \tag{1}$$

其中,δT_k 为梁的虚动能,δV_p 为梁的虚势能,δV_s 为梁两端支承弹簧的虚势能. 梁的虚动能的表达式为

$$\delta T_k = \int_0^L \rho A(W_{,T}\delta W_{,T} + U_{,T}\delta U_{,T})\,\mathrm{d}X \tag{2}$$

其中 $W(X,T)$ 和 $U(X,T)$ 分别表示梁的横向位移和纵向位移,由于纵向位移微弱,可以忽略不计. 梁的虚势能的表达式为

$$\delta V_p = \int_0^L\int_A \sigma\delta\varepsilon\,\mathrm{d}A\,\mathrm{d}X - P\int_0^L(W_{,X}\delta W_{,X})\,\mathrm{d}X \tag{3}$$

其中 $\varepsilon(X,Z,T)$ 和 $\sigma(X,Z,T)$ 分别是非线性轴向 Lagrange 应变和轴向扰动正应力. 采用 Kelvin 黏弹性本构关系模型

$$\sigma = E\varepsilon + \alpha\varepsilon_{,T} = E\left(-ZW_{,XX} + \frac{1}{2}W^2_{,X}\right) + \alpha(-ZW_{,XXT} + W_{,X}W_{,XT}) \tag{4}$$

其中,Z 为垂直于轴向坐标的竖向坐标,α 为黏性阻尼. 边界支承弹簧的势能为

$$V_s = \frac{1}{2}K_L\left[W(X,T)\right]^2\Big|_{X=0} + \frac{1}{2}K_R\left[W(X,T)\right]^2\Big|_{X=L} \tag{5}$$

将式(2)、式(3)和式(5),代入式(1)并变分得到弹性支承梁非线性振动的偏微分-积分控制方程

$$\rho AW_{,TT} + PW_{,XX} + EIW_{,XXXX} + \alpha IW_{,XXXXT} = \frac{1}{2L}W_{,XX}\int_0^L\left[EA\,(W_{,X})^2 + \alpha A(W_{,X}W_{,XT})\right]\mathrm{d}X \tag{6}$$

相应边界条件

$$\begin{aligned}
&K_LW(0,T) + EIW_{,XXX}(0,T) + PW_{,X}(0,T) = 0,\\
&K_RW(L,T) - EIW_{,XXX}(L,T) - PW_{,X}(L,T) = 0,\\
&W_{,XX}(0,T) = 0, W_{,XX}(L,T) = 0
\end{aligned} \tag{7}$$

引入下列无量纲参数

$$\begin{aligned}
&w = \frac{W}{L},\ x = \frac{X}{L},\ t = \frac{T}{L}\sqrt{\frac{E}{\rho}},\\
&k_f = \frac{1}{L}\sqrt{\frac{I}{A}},\ \mu = \frac{\alpha}{L}\sqrt{\frac{1}{E\rho}},\\
&p = \frac{P}{AE},\ \omega_b = \omega_B L\sqrt{\frac{\rho}{E}},\\
&k_L = \frac{K_\mathrm{L}L^3}{EI},\ k_R = \frac{K_\mathrm{R}L^3}{EI}
\end{aligned} \tag{8}$$

代入式(7)可以得到下式所示的无量纲控制方程和无量纲边界条件

$$w_{,tt} + pw_{,xx} + k_f^2w_{,xxxx} + k_f^2\mu w_{,xxxxt} = \frac{1}{2}w_{,xx}\int_0^1 w_{,x}^2dx \tag{9}$$

$$\begin{aligned}
&k_Lu(0,t) + w_{,xxx}(0,t) + \frac{p}{k_f^2}w_{,x}(0,t) = 0,\\
&k_Ru(1,t) - w_{,xxx}(1,t) - \frac{p}{k_f^2}w_{,x}(1,t) = 0,\\
&w_{,xx}(0,t) = 0, w_{,xx}(1,t) = 0
\end{aligned} \tag{10}$$

2 模态及频率

严格满足非线性偏微分方程的解是几乎不可能得到的,按照动力学经典方法,首先基于线性派生系统,求得满足边界的模态函数,因此忽略控制方程中的非线性项、阻尼项,得到系统的线性派生方程及其边界条件

$$\begin{aligned}
&w_{,tt} + k_f^2w_{,xxxx} + pw_{,xx} = 0\\
&k_Lw(0,t) + w_{,xxx}(0,t) + \frac{p}{k_f^2}w_{,x}(0,t) = 0,\\
&k_Rw(1,t) - w_{,xxx}(1,t) - \frac{p}{k_f^2}w_{,x}(1,t) = 0,\\
&w_{,xx}(0,t) = 0, w_{,xx}(1,t) = 0
\end{aligned} \tag{11}$$

假设梁横向自由振动的解为:

$$w(x,t) = \varphi(x)\sin\,(\omega t + \theta) \tag{12}$$

式中,ω 为固有频率,θ 为初相角,$\phi(x)$ 为模态函数,且其表达式为

$$\phi(x) = \mathrm{e}^{\lambda x} \tag{13}$$

其中 λ 为特征值. 将式(12)和式(13)代入线性派生方程式(11)得到特征方程

$$k_f^2\lambda^4 + p\lambda^2 - \omega^2 = 0 \tag{14}$$

由式(14)可以解得特征值,将特征值写成

$$\lambda_{1,2} = \pm\,\mathrm{i}\beta_1, \lambda_{3,4} = \pm\beta_2 \tag{15}$$

$$\beta_1 = \sqrt{\frac{p + \sqrt{p^2 + 4k_f^2\omega^2}}{2k_f^2}},\quad \beta_2 = \sqrt{\frac{-p + \sqrt{p^2 + 4k_f^2\omega^2}}{2k_f^2}} \tag{16}$$

假定梁的自由振动的模态为:

$$\phi(x) = C_1\cos\beta_1x + C_2\sin\beta_1x + C_3\mathrm{ch}\beta_2x + C_4\mathrm{sh}\beta_2x \tag{17}$$

其中 $C_j(j=1,2,3,4)$ 为模态系数,通过边界条件求出.

$$\begin{pmatrix}
k_L & -\beta_1^3 + \dfrac{k_1\beta_1}{k_f^2} & k_L & \beta_2^3 + \dfrac{k_1\beta_2}{k_f^2}\\
-\cos\,(\beta_1)\beta_1^2 & -\sin\,(\beta_1)\beta_1^2 & \cosh\,(\beta_2)\beta_2^2 & \sinh\,(\beta_2)\beta_2^2\\
H_{31} & H_{32} & H_{33} & H_{34}\\
-\beta_1^2 & 0 & \beta_2^2 & 0
\end{pmatrix}
\begin{pmatrix} C_1\\ C_2\\ C_3\\ C_4\end{pmatrix} = 0 \tag{18}$$

$$
\begin{aligned}
H_{31} &= k_R\cos(\beta_1) - \beta_1^3\sin(\beta_1) + \frac{p\sin(\beta_1)\beta_1}{k_f^2},\\
H_{32} &= k_R\sin(\beta_1) + \beta_1^3\cos(\beta_1) - \frac{p\cos(\beta_1)\beta_1}{k_f^2},\\
H_{33} &= k_R\cosh(\beta_2) - \beta_2^3\sinh(\beta_2) - \frac{p\sinh(\beta_2)\beta_2}{k_f^2},\\
H_{34} &= k_R\sinh(\beta_2) - \beta_2^3\cosh(\beta_2) - \frac{p\cosh(\beta_2)\beta_2}{k_f^2}
\end{aligned} \tag{19}
$$

解得

$$
\begin{aligned}
C_1 &= C_1,\\
C_2 &= \left\{-\frac{\beta_1^2\beta_2^3k_f^2\cos(\beta_1) - \beta_1^2\beta_2^3k_f^2\cosh(\beta_2) + k_Lk_f^2\beta_1^2\sinh(\beta_2)}{\beta_1\beta_2[\sin(\beta_1)\beta_1\beta_2^2k_f^2 - \sinh(\beta_2)\beta_1^2\beta_2k_f^2 + \sin(\beta_1)\beta_1k_1 + \sinh(\beta_2)\beta_2k_1]} + \right.\\
&\quad \left.\frac{k_Lk_f^2\beta_2^2\sinh(\beta_2) + \beta_1^2\beta_2k_1\cos(\beta_1) - \beta_1^2\beta_2k_1\cosh(\beta_2)}{\beta_1\beta_2[\sin(\beta_1)\beta_1\beta_2^2k_f^2 - \sinh(\beta_2)\beta_1^2\beta_2k_f^2 + \sin(\beta_1)\beta_1k_1 + \sinh(\beta_2)\beta_2k_1]}\right\}C_1,\\
C_3 &= \frac{\beta_1^2}{\beta_2^2}C_1,\\
C_4 &= \left\{-\frac{\beta_1^3\beta_2^2k_f^2\cos(\beta_1) - \beta_1^3\beta_2^2k_f^2\cosh(\beta_2) + k_Lk_f^2\beta_1^2\sin(\beta_1)}{\beta_1^{-1}\beta_2^3[\sin(\beta_1)\beta_1\beta_2^2k_f^2 - \sinh(\beta_2)\beta_1^2\beta_2k_f^2 + \sin(\beta_1)\beta_1k_1 + \sinh(\beta_2)\beta_2k_1]} + \right.\\
&\quad \left.\frac{k_Lk_f^2\beta_2^2\sin(\beta_1) - \beta_1\beta_2^2k_1\cos(\beta_1) + \beta_1\beta_2^2k_1\cosh(\beta_2)}{\beta_1^{-1}\beta_2^3[\sin(\beta_1)\beta_1\beta_2^2k_f^2 - \sinh(\beta_2)\beta_1^2\beta_2k_f^2 + \sin(\beta_1)\beta_1k_1 + \sinh(\beta_2)\beta_2k_1]}\right\}C_1
\end{aligned} \tag{20}
$$

其中 C_1 为非零常数. 如果存在非平凡解,那么系数矩阵行列式值为零,由此求得系统的固有频率.

表 1 给出了本文研究的梁的物理参数值以及几何参数值.

表 1　梁的材料参数

Table 1　Material parameters of the beam

Name	Notation	Value
Elastic modulus	E	68.9 GPa
Density	ρ	2880 kg/m^3
Length	L	0.5 m
Height	h	0.005 m
Bottom length	b	0.02 m
Damping	α μ	1.389×10^{-7} N s/m^2 2
Sectional area	A	1×10^{-4} m^2
Moment of inertia	I	2.083×10^{-10} m^4
Bending stiffness	k_{f}	0.00288675

图 2 给出了在不同支撑弹簧刚度下,系统第一阶固有频率随轴向张力的变化情况. 可以看出,随着轴向张力的增加,梁的固有频率逐渐减小. 当梁的第一阶固有频率为零时,结构发生静态失稳(又称屈曲失稳),此时对应的轴向力称为临界轴力. 由图 2 中可知对应的临界轴力如表 2 所示:

表 2　不同支撑刚度对应的临界轴力

Table 2　The critical axial force of different stiffnesses

k_L	k_R	$P_{cr}(N)$
100	100	566
70	70	
50	50	
30	30	

表 2 的结果表明,对称支撑条件下,弹簧刚度的大小对临界轴力没有影响.

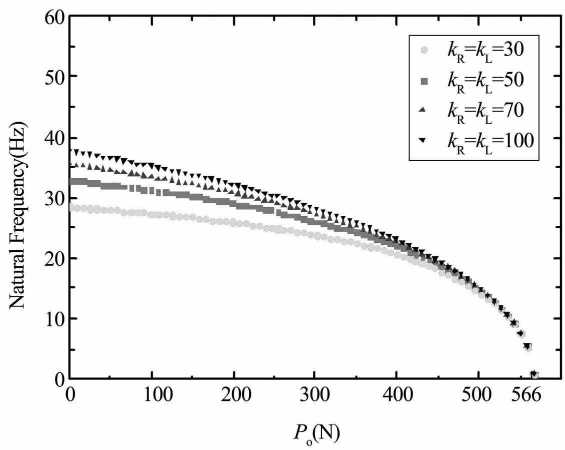

图 2　不同支撑刚度下的第一阶固有频率

Fig. 2　The first natural frequencies of different supporting stiffnesses

3 Galerkin 截断

采用 n 阶 Galerkin 截断,将梁的横向位移用广义坐标的形式表示为:

$$w(x,t) = \sum_{k=1}^{4} q_k(t)\phi_k(x) \tag{21}$$

其中,$q_n(t)$ 为梁的广义位移,模态函数 $\phi_n(t)$ 为特征函数. 权函数取特征函数本身,将广义坐标形式的位移函数(21)代入弹性支承梁的偏微分 - 积分控制方程,得到 n 个常微分方程

$$\begin{aligned}
&\int_0^1 \sum_{k=1}^{4} q''_k(t)\phi_k(x)\phi_m(x)\mathrm{d}x + \\
&p\int_0^1 \sum_{k=1}^{4} q_k(t)\phi''_k(x)\phi_m(x)\mathrm{d}x + \\
&k_f^2\int_0^1 \sum_{k=1}^{4} q_k(t)\phi''''_k(x)\phi_m(x)\mathrm{d}x + \\
&k_f^2\mu\int_0^1 \sum_{k=1}^{4} q'_k(t)\phi''''_k(x)\phi_m(x)\mathrm{d}x = \\
&\frac{1}{2}\int_0^1 \sum_{k=1}^{4} q_k(t)\phi_m(x)\phi(x)\mathrm{d}x \\
&\int_0^1 \left\{\sum_{k=1}^{4}\left[q_k(t)\phi'_k(x)\right]\right\}^2\mathrm{d}x, m = 1,2,3,4
\end{aligned} \tag{22}$$

设无量纲轴力在平均值附近做微小简谐脉动:

$$p = p_0 + p_1\cos(\omega_b t) \tag{23}$$

定义如下参数

$$\begin{aligned}
&C_{1m} = \\
&\frac{k_f^2\int_0^1 \sum_{k=1}^{4}\phi''''_k(x)\phi_m(x)\mathrm{d}x + p_0\int_0^1 \sum_{k=1}^{4}\phi''_k(x)\phi_m(x)\mathrm{d}x}{\int_0^1 \sum_{k=1}^{4}\phi_k(x)\phi_m(x)\mathrm{d}x}, \\
&C_{2m} = \frac{k_f^2\mu\int_0^1 \sum_{k=1}^{4}\phi''''_k(x)\phi_m(x)\mathrm{d}x}{\int_0^1 \sum_{k=1}^{4}\phi_k(x)\phi_m(x)\mathrm{d}x}, \\
&C_{3m} = \frac{p_1\int_0^1 \sum_{k=1}^{4}\phi''_k(x)\phi_m(x)\mathrm{d}x}{\int_0^1 \sum_{k=1}^{4}\phi_k(x)\phi_m(x)\mathrm{d}x}, \\
&C_{4m} = \frac{1}{2}\frac{\int_0^1 \sum_{k=1}^{4}\phi''0_k(x)\phi_m(x)\mathrm{d}x}{\int_0^1 \sum_{k=1}^{4}\phi_k(x)\phi_m(x)\mathrm{d}x}, \\
&N_{km} = \int_0^1 \sum_{k=1}^{4}\left[\phi'_k(x)\phi'_m(x)\right]\mathrm{d}x, \\
&k = 1,2,3,4, m = 1,2,3,4
\end{aligned} \tag{24}$$

整理得

$$\begin{aligned}
&q''_m + C_{1m}q_m + C_{2m}q'_m + C_{3m}q_m = \\
&q_m C_{4m}(2N_{13}q_1q_3 + 2N_{24}q_2q_4 + \sum_{k=1}^{4}N_{kk}q_k^2), \\
&m = 1,2,3,4
\end{aligned} \tag{25}$$

4 参激共振稳态响应

4.1 多尺度法分析过程

按照多尺度法过程,同时做如下代换:

$$q_m \leftrightarrow \varepsilon q_m,\ \alpha \leftrightarrow \varepsilon^2\alpha,\ p_1 \leftrightarrow \varepsilon^2 p_1 \tag{26}$$

整理得

$$\begin{aligned}
&q''_m + C_{1m}q_m + \varepsilon^2 C_{2m}q'_m + \varepsilon^2 C_{3m}\cos(\omega_b t)q_m = \\
&\varepsilon^2 q_m C_{4m}(2N_{13}q_1q_3 + 2N_{24}q_2q_4 + \sum_{k=1}^{4}N_{kk}q_k^2), \\
&m = 1,2,3,4
\end{aligned} \tag{27}$$

摄动解的形式设为:

$$q_m = q_{m0} + \varepsilon^2 q_{m2}, m = 1,2,3,4 \tag{28}$$

引入三个时间尺度

$$T_0 = \varepsilon^0 t, T_1 = \varepsilon^1 t,\ T_2 = \varepsilon^2 t \tag{29}$$

定义如下微分算子

$$\begin{aligned}
&\frac{\mathrm{d}T_0}{\mathrm{d}t} = \mathrm{D}_0, \frac{\partial}{\partial T_2} = \mathrm{D}_2, \\
&\frac{\mathrm{d}}{\mathrm{d}t} = \frac{\mathrm{d}T_0}{\mathrm{d}t}\frac{\partial}{\partial T_0} + \frac{\mathrm{d}T_2}{\mathrm{d}t}\frac{\partial}{\partial T_2} = \mathrm{D}_0 + \varepsilon^2\mathrm{D}_2, \\
&\frac{\mathrm{d}^2}{\mathrm{d}t^2} = \mathrm{D}_0^2 + 2\varepsilon^2\mathrm{D}_0\mathrm{D}_2 + \varepsilon^4\mathrm{D}_2^2
\end{aligned} \tag{30}$$

将式(28)、式(29)和式(30)代入式(27)得:

ε^0项系数.

$$\mathrm{D}_0^2 q_{m0} + C_{1m}q_{m0} = 0, m = 1,2,3,4 \tag{31}$$

ε^2项系数.

$$\begin{aligned}
&\mathrm{D}_0^2 q_{m2} + 2\mathrm{D}_0\mathrm{D}_2 q_{m0} + C_{2m}\mathrm{D}_0 q_{m0} + C_{1m}q_{m2} + \\
&C_{3m}\cos(\omega_b T_0)q_{m0} = C_{4m}q_{m0}(2N_{13}q_{10}q_{30} + \\
&2N_{24}q_{20}q_{40} + N_{11}q_{10}^2 + N_{22}q_{20}^2 + N_{33}q_{30}^2 + N_{44}q_{40}^2)
\end{aligned} \tag{32}$$

将式(31)解的形式设为

$$q_{m0} = A_m(T_2)\exp(\mathrm{i}\omega_m T_0) + cc, m = 1,2,3,4 \tag{33}$$

式中,cc 为前述项的共轭复数项. 将式(33)代入方程式(31)得

$$\omega_m = \sqrt{C_{1m}}, m = 1,2,3,4 \tag{34}$$

研究第 i 阶次谐波参数共振响应,由于参激振动会在外激励频率为二倍固有频率附近引发参激

响应,故引入解谐参数:

$$\omega_b = 2\omega_n + \varepsilon^2\sigma, n = 1,2,3,4 \tag{35}$$

将 ε^0 方程的解(33)和外激励频率(35)代入方程(32),提取长期项系数,即 $\exp(\mathrm{i}\omega_m T_0)$ 系数,可得

$$2\mathrm{i}\omega_m\left(\frac{\mathrm{d}}{\mathrm{d}T_2}A_m\right) + \frac{1}{2}\xi_{m,n}C_{3m}\bar{A}_m\mathrm{e}^{\mathrm{i}\sigma T_2} - A_m C_{4m}\left[\sum_{k=1}^{4}(2+\zeta_{m,k})A_k\bar{A}_k N_{kk}\right] + \mathrm{i}C_{2m}\omega_m A_m = 0 \tag{36}$$

$$\xi_{m,n} = \begin{cases}0, n \neq m \\ 1, n = m\end{cases}, \zeta_{m,k} = \begin{cases}0, k \neq m \\ 1, k = m\end{cases} \tag{37}$$

引入 A_m 的极坐标表达式

$$A_m(T_2) = \frac{1}{2}a_m(T_2)\mathrm{e}^{\mathrm{i}\theta_m(T_2)}, m = 1,2,3,4 \tag{38}$$

将解(38)代入式(37),并分离实部虚部

$$\frac{1}{4}\xi_{m,n}C_{3m}a_m\sin(\sigma T_2 - 2\theta_m) + \omega_m\left(\frac{\mathrm{d}}{\mathrm{d}T_2}a_m\right) + \frac{1}{2}a_m C_{2m}\omega_m = 0,$$

$$\frac{1}{4}\xi_{m,n}C_{3m}a_m\cos(\sigma T_2 - 2\theta_m) - \omega_m a_m\left(\frac{\mathrm{d}}{\mathrm{d}T_2}\theta_m\right) - \frac{1}{2}a_m C_{4m}\left[\sum_{k=1}^{4}\frac{(2+\zeta_{m,k})}{4}a_k^2 N_{kk}\right] = 0 \tag{39}$$

当系统做稳态运动时,系统幅值不再随时间变化

$$\frac{\mathrm{d}}{\mathrm{d}T_2}a_m = 0 \tag{40}$$

当 $m \neq i$ 时,即 $\xi_{m,i} = 0$ 时,解得

$$a_m = 0 \tag{41}$$

当 $m = i$ 时,即 $\xi_{m,i} = 1$ 时,做以下变量代换使方程组变成一个自治系统(即不显含 T_2 的系统)

$$\mathrm{e}^{\mathrm{i}[T_2\sigma - 2\theta_m(T_2)]} = \mathrm{e}^{\mathrm{i}\beta_m(T_2)}, (m = n) \tag{42}$$

当系统做稳态运动时,新相角不再随时间变化:

$$\frac{\mathrm{d}}{\mathrm{d}T_2}\beta_m = 0 \tag{43}$$

将式(40)、式(41)和式(43)代入方程组(39),整理得

$$\frac{1}{4}C_{3m}a_m\sin(\beta_m) + \frac{1}{2}C_{2m}a_m\omega_m = 0,$$

$$\frac{1}{4}C_{3m}a_m\cos(\beta_m) - \frac{1}{2}\omega_m a_m\sigma - \frac{3}{8}a_m^3 C_{4m}N_{mm} = 0 \tag{44}$$

消去方程(44)新相角得:

$$\frac{4C_{2m}^2\omega_m^2 + 4\omega_m^2\sigma^2 + 6\omega_m a_m^2\sigma C_{4m}N_{mm} + \frac{9}{4}a_m^4 C_{4m}^2 N_{mm}^2}{C_{3m}^2} = 1 \tag{45}$$

最终得到有量纲稳态横向位移的表达式为:

$$W(X,T) = L\sum_{m=1}^{4}q_m\varphi_m = L\sum_{m=1}^{4}a_m\cos(\omega_m T_0 + \theta_m)\varphi_m \tag{46}$$

用于数值计算的梁参数与表 1 相同,系统的初始轴力为 200 N,激励幅值为 60 N. Runge-Kutta 法数值计算时长取 1000 个周期,每个周期内取 50 个点,初始位移均取为 4×10^{-4},初始速度均取为 0.

图 3(a)和图 3(b)分别为 $k_L = k_R = 50$, $\omega_b = 2\omega_1 = 58.07$Hz 时的全局和局部时程图,可以看出此时系统已经进入稳态响应,仿真时长足够,取响应进入稳态最后一个周期响应的最大位移作为幅值,验证弹性梁稳态响应的近似解析解.

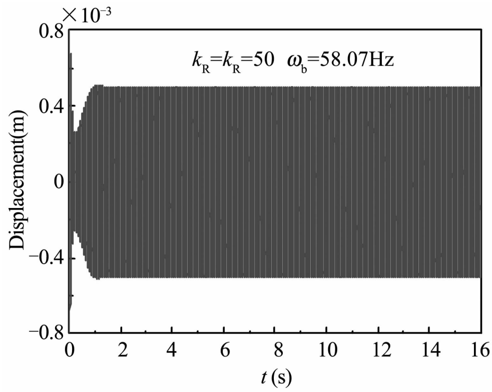

(a) 全局时程图
(a) Global time history

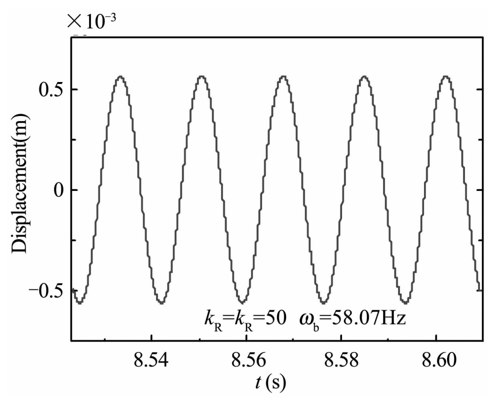

(b) 局部时程图
(b) Local time history

图 3　梁中点处稳态响应时程图
Fig. 3　Time history of steady-state response

图 4(a)和图(b)对比了两组刚度下通过二阶、四阶、六阶截断得到梁中点处稳态响应的数值仿真结果. 观察发现,二阶截断在共振区域边缘处,振幅较小时与四阶和六阶截断得到的结果差异较大,而四阶和六阶截断的结果吻合得很好,故本文后续研究均采用四阶截断,取 $n=4$.

图 5 利用 Runge-Kutta 法计算的数值解对多尺度近似解析结果进行了验证,图中实线代表近似解析解,散点代表数值仿真实验结果. 从图中的对比可以发现,近似解析解具有令人满意的计算精度,因此,本文接下来采用近似解析法对系统的动力学响应做进一步分析. 此外,由于立方非线性产生作用,且立方非线性项系数为正数,所以稳态响应共振峰向右偏移,系统呈现硬非线性特征.

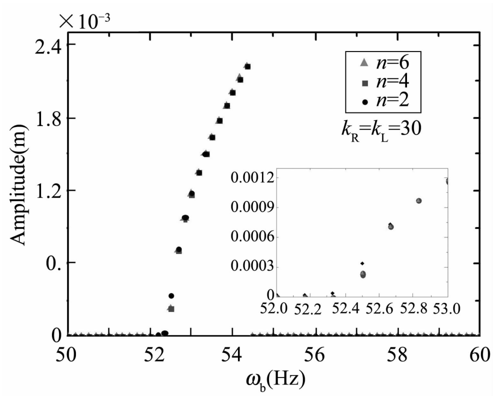

(a) $k_L = k_R = 30$ 时,梁中点处幅频图

(a) The amplitude of the midpoint at $k_L = k_R = 30$

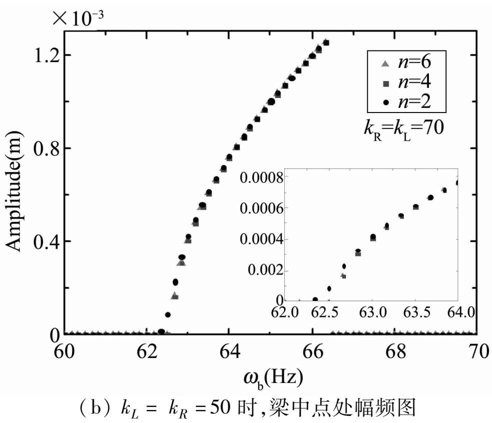

(b) $k_L = k_R = 50$ 时,梁中点处幅频图

(b) The amplitude of the midpoint at $k_L = k_R = 50$

图 4 不同截断阶数对比

Fig. 4 Comparison of different truncation orders

4.2 稳定性判断

为了研究零解的稳定性,按照 a_m 和 β_m 提取方程(43)左端的 Jacobian 矩阵,得到:

$$\begin{bmatrix} \frac{1}{4}C_{3m}\sin(\beta_m)+\frac{1}{2}C_{2m}\omega_m & \frac{1}{4}C_{3m}\cos(\beta_m) \\ \frac{1}{4}C_{3m}\cos(\beta_m)-\frac{1}{2}\omega_m\sigma & -\frac{1}{4}C_{3m}\sin(\beta_m) \end{bmatrix} \tag{47}$$

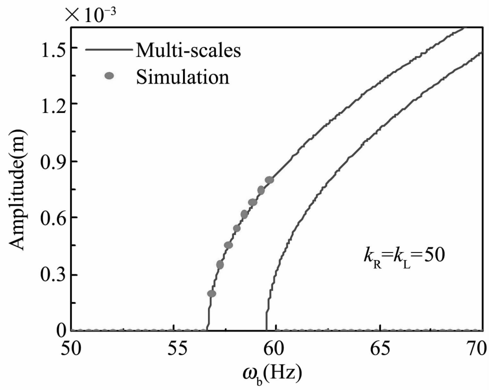

图 5 梁中点处幅频响应解析与数值结果对比

Fig. 5 Comparison of analytical and numerical results

根据 Routh-Hurwitz 判据,可以得出二次代数特征方程根不包含正实部的充分必要条件是特征方程中所有的系数均为正数,可得:

$$-\left[\frac{1}{4}C_{3m}\sin(\beta_m)+\frac{1}{2}C_{2m}\omega_m\right]\left[\frac{1}{4}C_{3m}a_m\sin(\beta_m)\right]-\left[\frac{1}{4}C_{3m}a_m\cos(\beta_m)\right]\left[\frac{1}{4}C_{3m}\cos(\beta_m)-\frac{1}{2}\omega_m\sigma\right]>0 \tag{48}$$

化简得

$$-C_{3m}^3a_m-2C_{2m}C_{3m}a_m\omega_m\sin(\beta_m)+2C_{3m}a_m\omega_m\sigma\cos(\beta_m)>0 \tag{49}$$

消去 a_m 和 β_m 得

$$-C_{3m}^2+4C_{2m}^2\omega_m^2+4\omega_m^2\sigma^2>0 \tag{50}$$

解得

$$C_{3m}<2\omega_m\sqrt{\sigma^2+C_{2m}^2} \tag{51}$$

图 6 给出了支撑刚度 $K_L = K_R = 5741.67$ N/m ($k_L = k_R = 50$)时,阻尼系数对系统稳定区域的影响. 从图中可以看出,系统的稳定性随着阻尼的增大而增大,且越靠近共振区域影响越显著. 这表明提高系统的阻尼,不仅可以提高发生参激共振的阈值,而且在同样的脉动压力下,系统必然发生参激共振的带宽也会缩小. 图 7 给出了阻尼系数 $\alpha = 1.389\times10^{-7}$ N s/m^2($\mu=2$)时,支撑弹簧刚度对系统稳定区域的影响. 从图中可以看出,系统的稳定性随着刚度的增大而减小,且越远离共振区影响越显著. 这种趋势表明,适当降低两端约束的刚度对抑制参激共振是有利的,不仅可以提高参激共振的

阈值,还能在同样的激励条件下,显著减小系统必然产生参激响应的带宽.

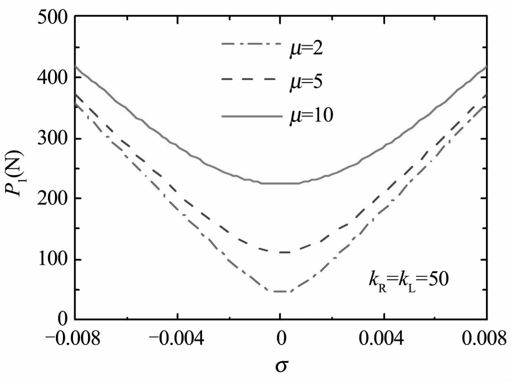

图 6　阻尼系数对系统稳定性的影响
Fig. 6　The influence of damping coefficient

图 8(a-c)分别给出了在不同支撑刚度、不同激励幅值以及不同平均轴力下系统共振区域附近的非线性响应,图 8(d)则展现了在平均轴力和支撑刚度共同作用下系统的非线性响应,其中虚线代表不稳定解,实线、点线与点划线代表稳定解. 从图 8(a)中可以看出,系统呈现出硬非线性特征,而随着支撑刚度的增大,系统的固有频率增大,共振区域向高频移动,发生共振的区间增大,同时系统的硬非线性特征增强. 由图 8(b)可以看出,随着激励幅值的增大,两支解的间距增大,系统发生共振的频率区间变大,在相同激励频率下,共振幅值也同时增大,系统的软硬特性不变. 由图 8(c)可见,当平均轴力增大时,共振区域向低频移动,发生共振的区间和共振幅值增大. 从图 8(d)中可以看出,当支撑刚度和平均轴力都较大时,系统的失稳区域较大,此时最易发生参激共振进而导致失稳.

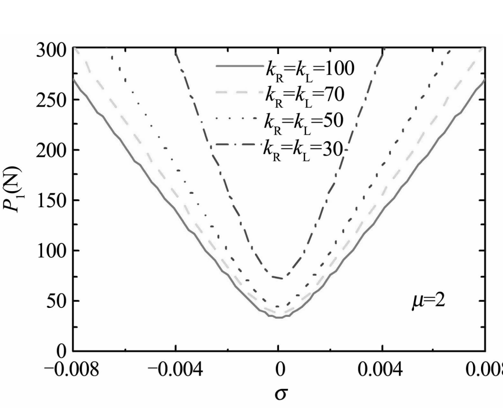

图 7　支撑弹簧刚度对系统稳定性的影响
Fig. 7　The influence of supporting spring stiffness

可以看出当两支解的间距越大,系统必然发生参激共振的区域越大,支撑刚度越小系统的稳定区域越大,这与上一小节中得到的结果相符,但还发现:减小支承刚度增大稳定区域的同时系统的共振幅值也会有所增大,这说明系统一旦发生参激共振,振动将会更加剧烈,在实际工程中需要更加注意. 而当外激励频率不变时,也可以通过改变支承刚度来避开共振区域以达到保护结构的目的. 对于激励幅值和平均轴力,系统稳定区域随其增大而减小,共振幅值随其增大而增大.

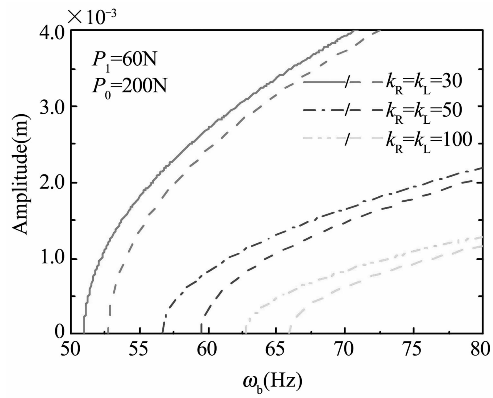

(a) 支撑刚度的影响
(a) The influence of support stiffness

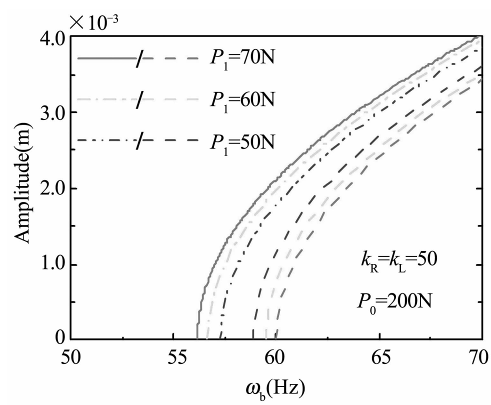

(b) 脉动激励幅值的影响
(b) The influence of excitation amplitude

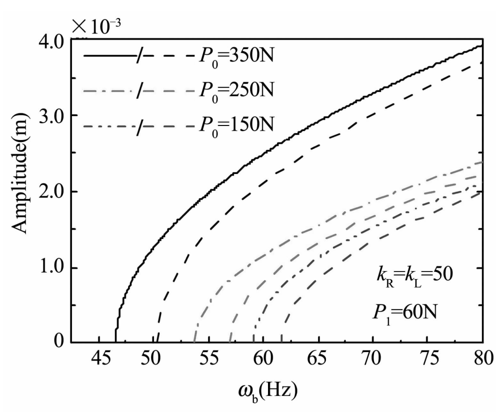

(c) 平均轴力的影响
(c) The influence of average axial force

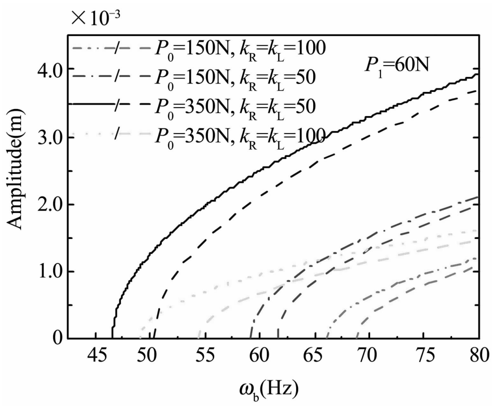

(d)平均轴力和支撑刚度共同影响
(d) The joint influence of average axial force and support stiffness

图8 系统参数对非线性响应的影响
Fig. 8 The influence of system parameters on nonlinear response

5 结论

本文以受轴向激励弹性支承梁为研究对象,采用Hamilton原理进行了动力学建模,并进行了模态分析,求得了系统固有频率. 然后利用Galerkin截断方法分别与多尺度法和Runge-Kutta方法结合,求得了近似解析解与数值解,并基于这两种结果分析了激励幅值、弹簧支撑刚度和平均轴向张力对系统非线性响应的影响. 之后根据求得的近似解析解,通过Routh-Hurwitz稳定性判据,得到了系统在不同阻尼系数和支撑弹簧刚度下的稳定边界,并进行了数值验证. 经过研究发现,系统的固有频率会随轴向压力的增大而减小,随着支撑弹簧刚度的增大而增大,但是使系统发生失稳的临界轴力并不会随对称的支撑弹簧刚度发生变化;增大阻尼系数可以增大系统的稳定区域,并且越靠近共振频率,阻尼系数的改变所产生的影响越大;减小支撑弹簧刚度将增大系统的零解稳定区域,且越偏离共振频率,弹簧刚度的改变所产生的影响越大;整个非线性系统呈现硬特性,随着支撑刚度的增加或平均轴力的减小,系统的硬特性增强. 而随着支撑刚度的减小、平均轴力的增大或激励幅值的增大,系统的共振幅值增大. 总之,以上研究结果将为工程中大量存在的弹性体稳定性设计提供理论指导.

参 考 文 献

1 方秦,杜茂林. 爆炸载荷作用下弹性与阻尼支撑梁的动力响应. 力学与实践,2006,28(2):53~56 (Fang Q, Du M L. Dynamic responses of an elastically supported beams with damping subjected to blast loads. *Mechanics in Engineering*,2006, 28(2): 53~56(in Chinese))

2 陈万祥,郭志昆. 粘弹性边界梁在低速冲击下的动力响应分析. 振动与冲击, 2008,27(12):69~72, 78 (Chen W X, Guo Z K. Dynamic responses of beams with the flexible supports subjected to low velocity impact. *Journal of Vibration and Shock*,2008, 27(12): 69~72, 78(in Chinese))

3 莫帅. 汽车荷载作用下弹性支承梁桥的动力响应分析[硕士学位论文]. 广州:暨南大学, 2014: 11~32 (Mo S. Dynamic response of elastic support bridge due to moving vehicles [Master Thesis]. Guangzhou: Jinan University, 2014:11~32(in Chinese))

4 Ding H, Ji J C, Chen L Q. Nonlinear vibration isolation for fluid-conveying pipes using quasi-zero stiffness characteristics. *Mechanical Systems and Signal Processing*, 2019, 121: 675~688

5 Ibrahim R A. Mechanics of pipes conveying fluids-Part II: Applications and fluid elastic problems. *Journal of Pressure Vessel Technology-Transactions of the ASME*, 2011: 133(2)

6 Ibrahim R A. Overview of mechanics of pipes conveying fluids-Part I: Fundamental studies. *Journal of Pressure Vessel Technology-Transactions of the ASME*, 2010: 132(3): 034001

7 Mao X Y, Ding H, Chen L Q. Steady-state response of a fluid-conveying pipe with 3:1 internal resonance in supercritical regime. *Nonlinear Dynamics*,2016, 86(2):795~809

8 Tan X, Mao X Y, Ding H, et al. Vibration around non-trivial equilibrium of a supercritical Timoshenko pipe conveying fluid. *Journal of Sound and Vibration*,2018, 428: 104~118

9 Tan X, Ding H, Chen L Q. Nonlinear frequencies and forced responses of pipes conveying fluid via a coupled Timoshenko model. *Journal of Sound and Vibration*, 2019, 455:241~255

10 Tan X, Ding H, Sun J Q, et al. Primary and super-harmonic resonances of Timoshenko pipes conveying high-speed fluid. *Ocean Engineering*,2020, 203: 107258

11 Kang K H, Kim K J. Modal properties of beams and plates on resilient supports with rotational and translational complex stiffness. *Journal of Sound and Vibration*, 1996, 190(2): 207~220

12 夏季,朱目成,马德毅. 带集中质量和弹性支撑梁的横向固有振动分析. 力学与实践. 2000, 22(5): 27 ~ 30 (Xia J, Zhu M C, Ma D Y. Analysis of lateral natural vibration of beams with lumped masses and elastic supports. *Mechanics in Engineering*, 2000, 22(5): 27 ~ 30 (in Chinese))

13 Li W L. Dynamic analysis of beams with arbitrary elastic supports at both ends. *Journal of Sound and Vibration*, 2001, 246(4): 751 ~ 756

14 Li W L. Vibration analysis of rectangular plates with general elastic boundary supports. *Journal of Sound and Vibration*, 2004, 273(3): 619 ~ 635

15 Li W L, Zhang X F, Du J T, et al. An exact series solution for the transverse vibration of rectangular plates with general elastic boundary supports. *Journal of Sound and Vibration*, 2009, 321(1 - 2): 254 ~ 269

16 Li Z Z, Tang D G, Li W W. Analysis of vibration frequency characteristic for elastic support beam. *Advanced Materials Research*, 2013, 671 - 674(2): 1324 ~ 1328

17 Gan B S, Kien N D, Ha L T. Effect of intermediate elastic support on vibration of functionally graded Euler-Bernoulli beams excited by a moving point load. *Journal of Asian Architecture and Building Engineering*, 2017, 16 (2): 363 ~ 369

18 Ding H, Zhu M H, Chen L Q. Nonlinear vibration isolation of a viscoelastic beam. *Nonlinear Dynamics*, 2018, 92(2): 325 ~ 349

19 Ding H, Li Y, Chen L Q. Nonlinear vibration of a beam with asymmetric elastic supports. *Nonlinear Dynamics*, 2019, 95(3): 2543 ~ 2554

20 Chen L Q, Chen H, Ding H, et al. Nonlinear combination parametric resonance of axially accelerating viscoelastic strings constituted by the standard linear solid model. *Science China-Technological Sciences*, 2010(03): 645 ~ 655

21 Ding H, Huang L L, Dowell E H, et al. Stress distribution and fatigue life of nonlinear vibration of an axially moving beam. *Science China-Technological Sciences*, 2019, 62(7): 1123 ~ 1133

22 Tang Y Q, Zhou Y, Liu S, et al. Complex stability boundaries of axially moving beams with interdependent speed and tension. *Applied Mathematical Modelling*, 2021, 89(1): 208 ~ 224

23 Liu J J, Li C, Yang C J, et al. Dynamical responses and stabilities of axially moving nanoscale beams with time-dependent velocity using a nonlocal stress gradient theory. *Journal of Vibration and Control*, 2017 23(20): 3327 ~ 3344

24 Mao X Y, Ding H, Chen L Q. Forced vibration of axially moving beam with internal resonance in the supercritical regime. *International Journal of Mechanical Sciences*, 2017, 131: 81 ~ 94

25 刘金建,蔡改改,谢锋,等. 轴向运动功能梯度粘弹性梁横向振动的稳定性分析. 动力学与控制学报, 2016 (6):533 ~ 541 (Liu J J, Cai G G, Xie F, et al. Stability analysis on transverse vibration of axially moving functionally graded viscoelastic beams. *Journal of Dynamics and Control*, 2016(6):533 ~ 541(in Chinese))

26 李炀,谭霞,丁虎,等. 两端带有弹簧支撑的轴向运动梁振动分析. 动力学与控制学报, 2019(4):45 ~ 50 (Li Y, Tan X, Ding H, et al. Nonlinear transverse vibration of an axially moving beam with vertical spring boundary. *Journal of Dynamics and Control*, 2019(4): 45 ~ 50(in Chinese))

27 Shaker F J. Effect of axial load on mode shapes and frequencies of beams. NASA Technical Note (NASA-TN-8109), 1975

28 Bokaian A. Natural frequencies of beams under compressive axial loads. *Journal of Sound and Vibration*, 1988, 126(1): 49 ~ 65

29 Bokaian A. Natural frequencies of beams under tensile axial loads. *Journal of Sound and Vibration*, 1990, 142 (3): 481 ~ 498

30 Kukla S. Free-vibrations of axially loaded beams with concentrated masses and intermediate elastic supports. *Journal of Sound and Vibration*, 1994, 172(4): 449 ~ 458

31 Matsunaga H. Free vibration and stability of thin elastic beams subjected to axial forces. *Journal of Sound and Vibration*, 1996, 191(5): 917 ~ 933

32 Luo Y Y. Frequency analysis of infinite continuous beam under axial loads. *Journal of Sound and Vibration*, 1998, 213(5): 791 ~ 800

33 Ji J C, Hansen C H. Non-linear response of a post-buckled beam subjected to a harmonic axial excitation. *Journal of Sound and Vibration*, 2000, 237(2): 303 ~ 318

34 Naguleswaran S. Transverse vibration of a uniform Euler-Bernoulli beam under linearly varying axial force. *Journal of Sound and Vibration*, 2004, 275(1-2): 47 ~ 57

35 Liu M F, Chang T P. Vibration analysis of a magneto-elastic beam with general boundary conditions subjected to

axial load and external force. *Journal of Sound and Vibration*, 2005, 288(1-2): 399 ~ 411

36 Pratiher B, Dwivedy S K. Parametric instability of a cantilever beam with magnetic field and periodic axial load. *Journal of Sound and Vibration*, 2007, 305(4-5): 904 ~ 917

37 Yang J, Chen Y, Xiang Y, et al. Free and forced vibration of cracked inhomogeneous beams under an axial force and a moving load. *Journal of Sound and Vibration*, 2008, 312(1-2): 166 ~ 181

38 Li C, Lim C W, Yu J L, et al. Transverse vibration of pre-tensioned nonlocal nanobeams with precise internal axial loads. *Science China Technological Sciences*, 2011, 54(8): 2007 ~ 2013

39 Li M W. Analytical study on the dynamic response of a beam with axial force subjected to generalized support excitations. *Journal of Sound and Vibration*, 2015, 338: 199 ~ 216

40 Zhou K, Ni Q, Dai H L, et al. Nonlinear forced vibrations of supported pipe conveying fluid subjected to an axial base excitation. *Journal of Sound and Vibration*, 2020, 471: 115189

41 Zhao X. Forced vibration analysis of Timoshenko double-beam system under compressive axial load by means of Green's functions. *Journal of Sound and Vibration*, 2020, 464:115001

STABILITY ANALYSIS OF AXIALLY EXCITED BEAM WITH ELASTIC BOUNDARY *

Zhang Chi Mao Xiaoye Ding Hu† Chen Liqun

(*School of Mechanics and Engineering Science, Shanghai University, Shanghai* 200444, *China*)

Abstract For beams with elastic supports, influence of the spring stiffness on parametric stability boundary of an axially excited beam is presented for the first time. Here, based on Hamilton's principle, dynamic governing equation of the axially excited beam supported by linear springs on both sides is established. The natural frequencies of the beam with axial compression are calculated by the analytical method. The relationships between the stiffness of the supporting spring, the natural frequencies and the critical loading of the system are obtained. Based on Galerkin truncation, semi-analytical and numerical solutions of the steady-state response are obtained by the multi-scale method and the Runge-Kutta method. The effects of the excitation amplitude, supporting stiffness and the average axial force on the nonlinear response are discussed. The stability boundary of the parametric resonance is obtained by the Routh-Hurwitz stability criterion. The influence of the supporting stiffness and the damping on the stability of the parametric resonance are fully discussed. It is found that the stiffness of the supporting spring can significantly change the parametric stability boundary of the beam. Therefore, the results will provide guidelines for design of structures subjected to axial excitation.

Key words beam, elastic support, axial excitation, parametric resonance, nonlinear vibration, stability boundary

Received 14 April 2021, Revised 4 May 2021.

* The project supported by the National Natural Science Foundation for Distinguished Young Scholars of China (12025204).

† Corresponding author E-mail: dinghu3@ shu. edu. cn